5. External-field-driven flow

One of the simplest ways to implement time-dependent boundary conditions in SOMA is to apply time-dependent external fields that are only nonzero close to the boundaries and have the form:

$$E_i(\mathbf{r}, t) = f_i(\mathbf{r}, t)\phi_i(\mathbf{r}, t)\,, \tag{5.1}$$

where $i = \mathrm{A}, \mathrm{B}$ denotes the monomer types. In this section, layers of lamellar diblock-copolymers are moved at constant speed v perpendicular to their orientation using spatially periodic external fields close to the boundaries. In a system that moves along with the external field, each monomer experiences a friction force ζv in the opposite direction, where ζ is obtained from (2.5). The degree of deformation depends on the Péclet number $P_e \equiv vR_e/D$. For large values $P_e \approx 1$, the chains cannot keep up with the external field movement and the lamellae break. For small $P_e \approx 0$, they have enough time to fully relax to the undeformed shape. In this section, an intermediate regime is investigated to obtain the bending modulus K.

5.1. Reference system

A system of $n = 750$ symmetric diblock-copolymers with $N_A = N_B = N/2 = 16$ and $\chi N = 20$ is used. The box dimensions are $L_x \times L_y \times L_z = 2.5 \times 2.82 \times 1\, R_e^3$, which corresponds to $\sqrt{N} = 106$. The spatial discretizations are $\Delta x = 1/16\, R_e$, $\Delta y = 47/800\, R_e$ and $\Delta z = 1\, R_e$. To generate the initial lamellar structure, external fields are applied, as shown in Figure 5.1. The interlayer spacing of $d = 1.41\, R_e$ was found to be stable over the duration of the simulations, but it does not correspond to the equilibrium spacing.

Subsequently, the external fields are switched off everywhere except at a distance less than $b = 0.5\, R_e$ from the boundaries in the x-direction, so the length of the part

of the lamellae that is not supported by the external fields is $L = 1.5\,R_e$. Every Δt MCS, the fields are moved by a distance of Δy in the y-direction, so the velocity is $v = 47R_e/(800\Delta t)$. The external fields balance the friction forces at the boundaries and therefore act as bearings for the lamellae. The diffusion constant D is obtained from (2.7), where $g_3(t)$ is measured in a system without external fields and $\chi N = 0$.

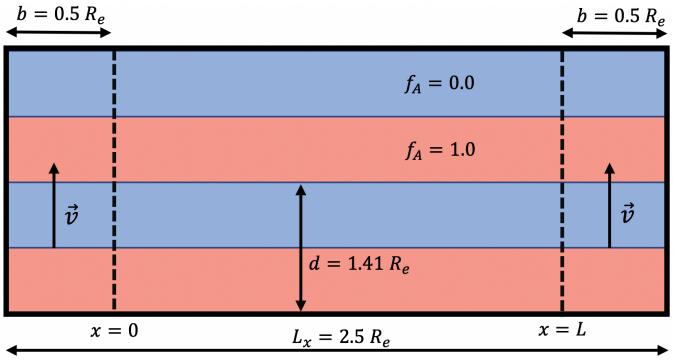

Figure 5.1.: Sketch of the external field $f_{\mathrm{A}}(\mathbf{r}, 0)$. Red domains correspond to $f_{\mathrm{A}} = 1.0$, blue domains to $f_{\mathrm{A}} = 0.0$. $f_{\mathrm{B}}(\mathbf{r}, 0)$ is exactly complementary. Within the region bounded by the dotted lines, the external fields are switched off after the initial lamella structure has been generated.

5.2. Bending modulus

For small deformations, in the SSL, the free energy of a bent lamella is [29]:

$$F = \int d\mathbf{r} \left\{ f_0 + \frac{1}{2} K \left(\partial_x^2 u\right)^2 \right\}, \tag{5.2}$$

$$\approx dL_z \int dx \left\{ f_0 + \frac{1}{2} K \left(\partial_x^2 u\right)^2 \right\}$$

$$\equiv dL_z \int dx f(u, u'')\,. \tag{5.3}$$

where f_0 is the free energy per unit volume of the unbent lamella, K is the bending modulus and $u \equiv u(x)$ is the deformation profile of the A-B-interface. For the integration over y and z, the change of volume was neglected. The friction force density is $q_{fric} = N\sqrt{\bar{N}}\zeta P_e D/R_e^4$. In the steady-state, it is balanced by a force density given by the functional derivative $\delta F/\delta u$:

$$\frac{\delta F}{\delta u} = q_{fric} = \frac{\partial^2}{\partial x^2}\frac{\partial f}{\partial u''}$$
$$\implies K\frac{\partial^4 u}{\partial x^4} = N\sqrt{\bar{N}}\zeta\frac{P_e D}{R_e^4}\,. \tag{5.4}$$

With the boundary conditions $u(0) = u(L) = 0$ and $u''(0) = u''(L) = 0$, one obtains:

$$u(x) = \frac{N\sqrt{\bar{N}}\zeta P_e D x}{24KR_e^4}(L^3 - 2L^2x + x^3)\,, \tag{5.5}$$

in analogy to a beam bending under a uniform load in the Euler-Bernoulli theory. The resulting lamella profile for $P_e = 0.24$ is shown in Figure 5.2. The fit is in excellent agreement with the simulation data.

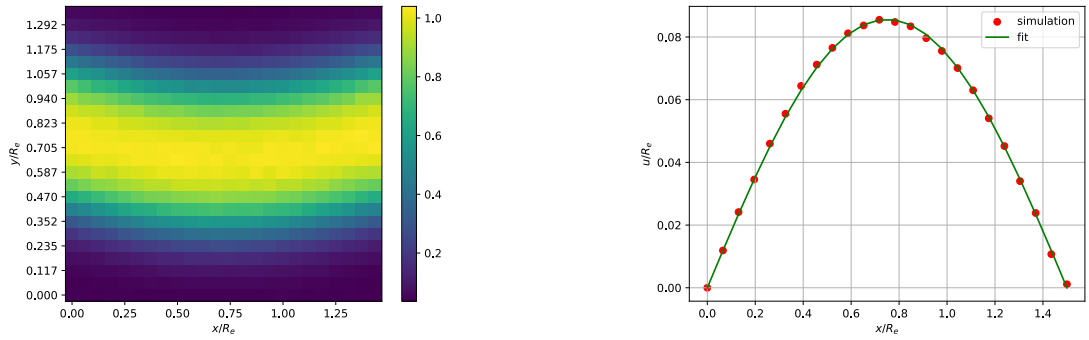

(a) (b)

Figure 5.2.: (a) Heatmap of the steady-state lamella profile in the reference frame that moves with the external field, averaged over all lamellae. (b) Lamella center of mass curve for $P_e = 0.34$. The fit corresponds to (5.5).

The maximum deformation is:

$$u_{max} = u(L/2) = \frac{5N\sqrt{\bar{N}}\zeta P_e D L^4}{384KR_e^4}\,. \tag{5.6}$$

To obtain the bending modulus, u_{max} is measured for various values of P_e, this is shown in Figure 5.3.

From (5.6), one obtains $K = 19.98\,k_BT/R_e$. Alternatively, K may also be obtained from exact SCFT. For this, the free energy of bending is computed for a

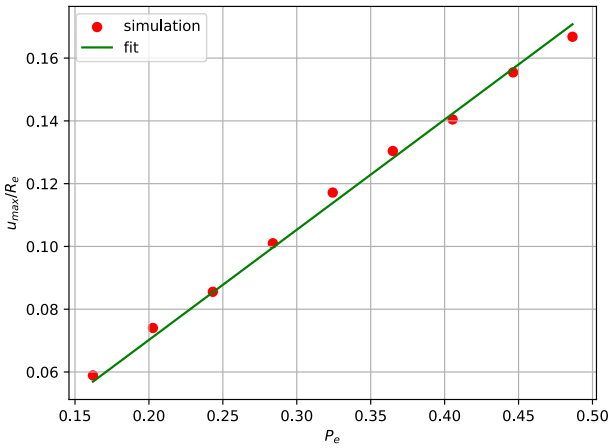

Figure 5.3.: Maximum deflection u_{max} as a function of the Péclet number P_e. The fit corresponds to (5.6).

sinusoidal deformation $u(x) = a \sin 2\pi x/L$, as shown in Figure 5.4. From (5.3), the total free energy may be calculated as:

$$\begin{aligned} F &= dL_z \int dx \left\{ f_0 + \frac{1}{2} K a^2 \left(\frac{2\pi}{L}\right)^4 \sin\left(\frac{2\pi}{L} x\right)^2 \right\} \\ &\approx dLL_z f_0 + dL_z \frac{4\pi^4 a^2}{L^3} K \,. \end{aligned} \tag{5.7}$$

On the other hand, the total free energy may be obtained by integrating over the free energy density:

$$\begin{aligned} F &= \int d\mathbf{r}(f_0 + f_b) \\ &\approx dLL_z(f_0 + f_b) \\ &= dLL_z \frac{\sqrt{\bar{N}}}{R_e^3}(\tilde{f}_0 + \tilde{f}_b) \,, \end{aligned} \tag{5.8}$$

where $\tilde{f}_0 = 4.0337\, k_B T$ is the free energy per chain of the undeformed lamella and $\tilde{f}_b = 0.79278\, k_B T (a/R_e)^2$ is the free energy per chain due to the deformation. Comparing (5.7) and (5.8), the bending modulus reads:

$$K_{\mathrm{SCFT}} = \frac{\tilde{f}_b \sqrt{\bar{N}}}{4a^2\pi^4} R_e^{-3} L^4 \,. \tag{5.9}$$

The result is $K_{\mathrm{SCFT}} = 17.47\, k_B T / R_e$, which is slightly smaller than the simulation result.

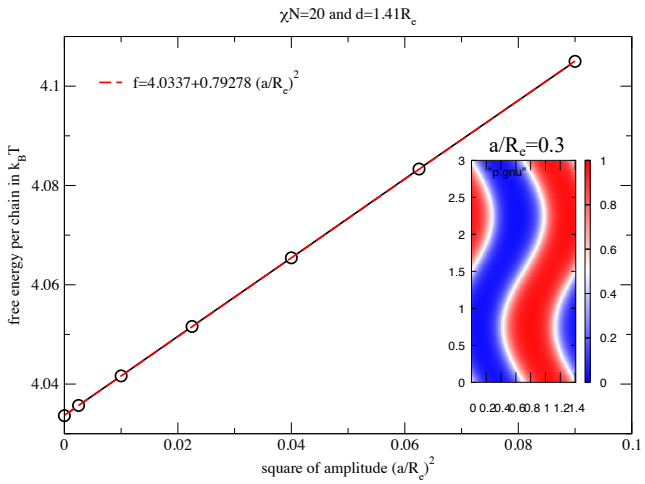

Figure 5.4.: Free energy per chain as a function of the square of the amplitude from exact SCFT calculations. The inset shows the lamella cross-section for $a/R_e = 0.3$.

Bibliography

[1] Optimization by simulated annealing. *Science*, 220(4598):671–680, 1983. doi: 10.1126/science.220.4598.671. URL https://www.science.org/doi/abs/10.1126/science.220.4598.671.

[2] J. Baschnagel, H. Meyer, F. Varnik, S. Metzger, M. Aichele, M. Müller, and K. Binder. Computer simulations of polymers close to solid interfaces: Some selected topics. *Interface Science*, 11(2):159–173, 2003. doi: 10.1023/A:1022118610890. URL https://doi.org/10.1023/A:1022118610890.

[3] Frank S. Bates, Wayne W. Maurer, Paul M. Lipic, Marc A. Hillmyer, Kristoffer Almdal, Kell Mortensen, Glenn H. Fredrickson, and Timothy P. Lodge. Polymeric bicontinuous microemulsions. *Phys. Rev. Lett.*, 79:849–852, Aug 1997. doi: 10.1103/PhysRevLett.79.849. URL https://link.aps.org/doi/10.1103/PhysRevLett.79.849.

[4] K. Binder. Collective diffusion, nucleation, and spinodal decomposition in polymer mixtures. *The Journal of Chemical Physics*, 79(12):6387–6409, 1983. doi: 10.1063/1.445747. URL https://doi.org/10.1063/1.445747.

[5] Kostas Ch. Daoulas and Marcus Müller. Single chain in mean field simulations: Quasi-instantaneous field approximation and quantitative comparison with monte carlo simulations. *The Journal of Chemical Physics*, 125(18):184904, 2006. doi: 10.1063/1.2364506. URL https://doi.org/10.1063/1.2364506.

[6] P. G. de Gennes. Dynamics of fluctuations and spinodal decomposition in polymer blends. *The Journal of Chemical Physics*, 72(9):4756–4763, 1980. doi: 10.1063/1.439809. URL https://doi.org/10.1063/1.439809.

[7] Oliver Dreyer, Gregor Ibbeken, Ludwig Schneider, Niklas Blagojevic, Maryam Radjabian, Volker Abetz, and Marcus Müller. Simulation of solvent evaporation from a diblock copolymer film: Orientation of the cylindrical mesophase.

Macromolecules, 55(17):7564–7582, 2022. doi: 10.1021/acs.macromol.2c00612. URL https://doi.org/10.1021/acs.macromol.2c00612.

[8] Dominik Düchs, Venkat Ganesan, Glenn H. Fredrickson, and Friederike Schmid. Fluctuation effects in ternary ab + a + b polymeric emulsions. *Macromolecules*, 36(24):9237–9248, 12 2003. doi: 10.1021/ma030201y. URL https://doi.org/10.1021/ma030201y.

[9] A. Einstein. Über die von der molekularkinetischen theorie der wärme geforderte bewegung von in ruhenden flüssigkeiten suspendierten teilchen. *Annalen der Physik*, 322(8):549–560, 1905. doi: https://doi.org/10.1002/andp.19053220806. URL https://onlinelibrary.wiley.com/doi/abs/10.1002/andp.19053220806.

[10] I Ya Erukhimovich and AN Semenov. Nonexponential density relaxation and the dynamic form-factor of polymer melts in the reptation regime. *Zh. Eksp. Teor. Fiz*, 63:275, 1986.

[11] Paul J. Flory. Thermodynamics of high polymer solutions. *The Journal of Chemical Physics*, 10(1):51–61, 1942. doi: 10.1063/1.1723621. URL https://doi.org/10.1063/1.1723621.

[12] J. G. E. M. Fraaije, B. A. C. van Vlimmeren, N. M. Maurits, M. Postma, O. A. Evers, C. Hoffmann, P. Altevogt, and G. Goldbeck-Wood. The dynamic mean-field density functional method and its application to the mesoscopic dynamics of quenched block copolymer melts. *The Journal of Chemical Physics*, 106(10):4260–4269, 1997. doi: 10.1063/1.473129. URL https://doi.org/10.1063/1.473129.

[13] Ludwik Leibler. Theory of microphase separation in block copolymers. *Macromolecules*, 13(6):1602–1617, 1980.

[14] R.H. Colby M. Rubinstein. *Polymer Physics*. Oxford University Press, 2003.

[15] Nicholas Metropolis, Arianna W. Rosenbluth, Marshall N. Rosenbluth, Augusta H. Teller, and Edward Teller. Equation of State Calculations by Fast Computing Machines. *The Journal of Chemical Physics*, 21(6):1087–1092, 12 2004. ISSN 0021-9606. doi: 10.1063/1.1699114. URL https://doi.org/10.1063/1.1699114.

[16] M. Müller and G. Gompper. Elastic properties of polymer interfaces: Aggregation of pure diblock, mixed diblock, and triblock copolymers. *Phys. Rev. E*, 66:041805, Oct 2002. doi: 10.1103/PhysRevE.66.041805. URL https://link.aps.org/doi/10.1103/PhysRevE.66.041805.

[17] Marcus Müller. Studying amphiphilic self-assembly with soft coarse-grained models. *Journal of Statistical Physics*, 145:967–1016, 11 2011. doi: 10.1007/s10955-011-0302-z.

[18] Marcus MÃ¼ller and Kostas Ch. Daoulas. Single-chain dynamics in a homogeneous melt and a lamellar microphase: A comparison between Smart Monte Carlo dynamics, slithering-snake dynamics, and slip-link dynamics. *The Journal of Chemical Physics*, 129(16), 10 2008. ISSN 0021-9606. doi: 10.1063/1.2997345. URL https://doi.org/10.1063/1.2997345. 164906.

[19] C. Pangali, M. Rao, and B.J. Berne. On a novel monte carlo scheme for simulating water and aqueous solutions. *Chemical Physics Letters*, 55(3): 413–417, 1978. ISSN 0009-2614. doi: https://doi.org/10.1016/0009-2614(78)84003-2. URL https://www.sciencedirect.com/science/article/pii/0009261478840032.

[20] C. Pangali, M. Rao, and B.J. Berne. On a novel monte carlo scheme for simulating water and aqueous solutions. *Chemical Physics Letters*, 55(3): 413–417, 1978. ISSN 0009-2614. doi: https://doi.org/10.1016/0009-2614(78)84003-2. URL https://www.sciencedirect.com/science/article/pii/0009261478840032.

[21] Shuanhu Qi and Friederike Schmid. Hybrid particle-continuum simulations coupling brownian dynamics and local dynamic density functional theory. *Soft Matter*, 13:7938–7947, 2017. doi: 10.1039/C7SM01749A. URL http://dx.doi.org/10.1039/C7SM01749A.

[22] Ellen Reister. *Zusammenhang zwischen der Einzelkettendynamik und der Dynamik von Konzentrationsfluktuationen in mehrkomponentigen Polymersystemen*. PhD thesis, Mainz, 2002.

[23] Peter J. Rossky, Jimmie D. Doll, and Harold L. Friedman. Brownian dynamics as smart monte carlo simulation. *Journal of Chemical Physics*, 69:4628–4633, 1978.

[24] Prince E. Rouse. A theory of the linear viscoelastic properties of dilute solutions of coiling polymers. *The Journal of Chemical Physics*, 21(7):1272–1280, 1953. doi: 10.1063/1.1699180. URL https://doi.org/10.1063/1.1699180.

[25] Ludwig Schneider and Marcus Müller. Multi-Architecture Monte-Carlo (MC) Simulation of Soft Coarse-Grained Polymeric Materials: SOft coarse grained Monte-carlo Acceleration (SOMA). *arXiv e-prints*, art. arXiv:1711.03828, November 2017. doi: 10.48550/arXiv.1711.03828.

[26] A. N. Semenov. Theory of Long-Range Interactions in Polymer Systems. *J. Phys. II*, 6(12):1759–1780, December 1996. ISSN 1155-4312. doi: 10.1051/jp2:1996159.

[27] Jörn Ilja Siepmann and Daan Frenkel. Configurational bias monte carlo: a new sampling scheme for flexible chains. *Molecular Physics*, 75(1):59–70, 1992. doi: 10.1080/00268979200100061. URL https://doi.org/10.1080/00268979200100061.

[28] Glenn M. Torrie and John P. Valleau. Monte carlo free energy estimates using non-boltzmann sampling: Application to the sub-critical lennard-jones fluid. *Chemical Physics Letters*, 28(4):578–581, 1974. ISSN 0009-2614. doi: https://doi.org/10.1016/0009-2614(74)80109-0. URL https://www.sciencedirect.com/science/article/pii/0009261474801090.

[29] Zhen-Gang Wang. Response and instabilities of the lamellar phase of diblock copolymers under uniaxial stress. *The Journal of Chemical Physics*, 100(3):2298–2309, 02 1994. ISSN 0021-9606. doi: 10.1063/1.466528. URL https://doi.org/10.1063/1.466528.